ORIGINAL PAPER

Crack in a lattice waveguide

**Leonid I. Slepyan · Alexander B. Movchan ·
Gennady S. Mishuris**

Abstract We consider some structures where the harmonic 'feeding' wave localized at the crack faces can force the crack to grow. First, we present some results related to a lattice with a high-contrast layer, where the wave speed is larger than in the ambient matrix. The analytical solution obtained for the steady-state regime, where the crack speed is independent of the wave amplitude, is used to determine the energy relations and the wave-amplitude-dependent position of the crack front relative to the feeding wave. The corresponding numerical simulations confirmed the existence of the steady-state regime within a range of the wave amplitude. For lager amplitudes the simulations revealed a set of ordered crack-speed oscillation regimes, where the average crack speed is characterized by a stepwise dependence on the wave amplitude. We show that the related cluster-type wave representation allows the average crack speeds to be determined analytically. We also show the connection between the cluster representation and the 'local'
crack-speeds within the cluster. As an example of a continuous system, where the crack can uniformly grow under the localized harmonic wave, an elastic flexural plate is considered. Both symmetric and anti-symmetric fracture modes are examined.

Keywords Dynamic fracture · Vibrations · Inhomogeneous material · Supersonic crack · Integral transforms

1 Introduction

We consider a semi-infinite crack in a two-dimensional elastic structure. The crack is assumed to grow while a harmonic wave is radiated by a localized remote source placed behind the crack front. The parameters of the lattice are chosen in such a way that the wave is localized at the crack faces and hence can reach the crack front. It is assumed that the crack moves uniformly and hence its speed coincides with the wave phase speed. In this steady-state regime, the group velocity of the wave, which is equal to the energy flux velocity, must exceed its phase speed; otherwise, the wave cannot deliver the energy to the crack front, as required to support the crack growth. Note that in principle, an opposite situation can exist where the crack gains the energy from the wave ahead of the crack front. In this latter case, the steady-state regime can exist if the group velocity of the wave is below its phase speed.

L. I. Slepyan (✉)
School of Mechanical Engineering, Tel Aviv University,
Tel Aviv, Israel
e-mail: leonid@eng.tau.ac.il

A. B. Movchan
Department of Mathematical Sciences, University
of Liverpool, Liverpool, UK

G. S. Mishuris
Institute of Mathematics and Physics, Aberystwyth University,
Aberystwyth, UK

The key role of the dispersion relations is emphasized in the lattice problem as well as in the problem for the flexural elastic plate. One of these dispersion relations corresponds to the half-plane with a traction-free boundary (the crack faces) and the other one corresponds to the symmetry condition (the crack continuation). Given the incident (feeding) wave frequency, the dispersion relations are used to determine the corresponding crack speed and the frequencies of the reflected and refracted waves.

The dynamic crack growth in a lattice under a non-localized harmonic wave was first considered by Slepyan (1981) (also see Slepyan 2002). In the previous paper by the authors (Mishuris et al. 2009), we considered the dynamic crack growth caused by a localized sinusoidal wave. In the wave-fracture scenario, the harmonic 'feeding wave' delivers energy to the moving crack front, while the reflected 'dissipative waves' carry a part of this energy away from the front. Two well established regimes were examined analytically: the steady-state regime, where the motion of neighboring masses (along the interface) differs only by a constant shift in time, and an alternating-strain regime, where the motion of neighboring masses also differs by sign. The energy of the localized reflective waves as well as the energy radiated to the ambient lattice were evaluated.

The numerical simulations conducted for a high-contrast interface confirm the theoretical findings for the above-mentioned regimes and, in addition, reveal some different, crack-speed oscillating regimes with a stepwise dependence of the averaged crack speed on the wave amplitude. A special attention is now given to such a locally irregular crack motion. In the numerical simulations, we consider a discrete chain with the local interaction of the particles, which is the limiting model for the corresponding 2D lattice with a high-contrast interface. For the corresponding periodic structure we find a set of dispersion relations for each value of the cluster width. For a general case, where the cluster contains n particles, the Floquet type wave can be represented as a superposition of n sinusoidal waves $u_q = u(q) \exp[\mathrm{i}(\omega t - km(q))]$, where the subscript q corresponds to the particle number within the cluster, $q = 1, 2, \ldots, n$, and $m(q) = q, q + n, q + 2n, \ldots$, is the discrete coordinate of the particle. If the dispersion relation for $n = 1$ is $f(\omega) = \cos k$, then for a general n there are n dispersion relations: $f(\omega) = \cos(k -$

$2\pi p/n)$, $p = 0, 1, \ldots, n - 1$, with the displacement amplitudes $u(q + 1) = u(q) \exp(2\pi \mathrm{i} p/n)$. It follows that the phase speed, averaged over the cluster, is equal to ω/k, whereas the local speeds can take different values.

The model for an elastic flexural plate gives an example of a continuous homogeneous structure which possesses special properties related to the considered type of fracture. Some aspects of the crack dynamics in the plate, including that interacting with a compressible fluid, are considered in Slepyan (2002, Sect. 9.7). In this model, the crack closure phenomenon can be important (see, e.g., Slepyan et al. 1995); in the present consideration, however, it is neglected.

The edge wave in the flexural plate half-plane is exponentially localized (in fact, rather weakly) having slightly lower phase and group velocities, v and $v_{\mathrm{g}} = 2v$, than the flexural wave in the plate in front of the crack. For the plate, both symmetric and antisymmetric modes of fracture are inspected. The energy criterion is used, and the ratio of the energy release rate to the energy delivered by the feeding wave is determined. This ratio appears to be very small especially for the symmetric mode. In contrary to the lattice, the dispersion relations define a unique crack speed independently of the wave amplitude, and this relations give no direct evidence concerning the existence of other ordered regimes.

Thus, the structure of the paper is as follows. We show that the localized feeding wave, which supplies the energy to the crack front, can exist in the case of a rather low contrast interface as well as for the case of high-contrast. Both types of the higher-wave-speed interface are considered: the one with lighter masses and the other one with stiffer bonds. The main steps in the analytical solution for the steady-state formulation are shown. Then we consider the results of the numerical simulation and identify a discrete set of the average crack speeds. We propose a theoretical framework for such regimes based on the cluster-type wave representation. It appears that the discrete values of the average crack speed, found numerically, are in agreement with the theoretical prediction of the possible speed.

Finally, we note that a flexural plate gives an example of a continuous body where the group velocity of the edge wave exceeds its phase velocity, and the growth of the steady-state dynamic crack can be supported by the localized sinusoidal wave.
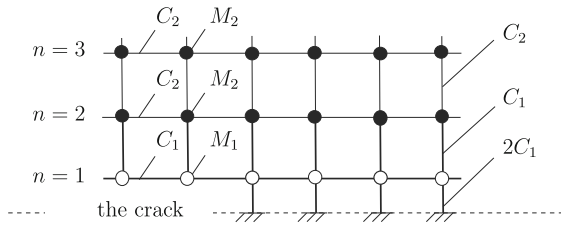
Fig. 1 The lattice with the propagating crack. The upper part of the symmetric structure is shown. The structural interface consists of two rows, $n = 1$ and $n = -1$ (the latter is not shown), of masses M_1 connected with each other and with the ambient lattice by the massless bonds of the stiffness C_1. Since the displacements are antisymmetric with respect to n, the middle point of each bond between $n = 1$ and $n = -1$ is fixed. Thus, the effective stiffness of this bond is $2C_1$

2 The lattice waveguide

2.1 The lattice

As in the paper by Mishuris et al. (2009) mode III dynamic fracture of a square lattice shown in Fig. 1 is considered. The lattice consists of point masses M_1, M_2, connected by linearly elastic bonds of stiffnesses C_1, C_2. The particles of the mass M_1, together with the bonds of the stiffness C_1, form the structured interface. Given (m, n) as a multi-index characterizing a position of a mass within the lattice, the structured interface consists of the masses at $n = \pm 1$, and the bonds between these rows and between the rows $n = \pm 1$ and $n = \pm 2$, respectively. The ambient lattice lies above and below the interface; it consists of the rows $n = \pm 2, \pm 3, \ldots,$ and the corresponding bonds connected neighboring rows. The normalization is introduced in such a way that the lattice spacing, the mass M_2 and the stiffness C_2 are equal to unity. In the steady-state regime, the crack is assumed to propagate between the rows $n = 1$ and $n = -1$, with a constant speed v. This implies that the time interval between the breakages of neighboring bonds is equal to $1/v$. Due to the symmetry of the problem, we can consider only the part of the lattice located in the upper half-plane, as shown in Fig. 1.

The equations of motion of the intact lattice have the form:

$$M_1 \ddot{u}_{m,1}(t) = C_1[u_{m+1,1}(t) + u_{m-1,1}(t)$$
$$+ u_{m,2}(t) - \beta u_{m,1}(t)],$$
$$\ddot{u}_{m,2}(t) = [u_{m+1,2}(t) + u_{m-1,2}(t) + u_{m,3}(t)$$
$$- 3u_{m,2}(t)] + C_1[u_{m,1}(t) - u_{m,2}(t)],$$

$$\ddot{u}_{m,n}(t) = [u_{m+1,n}(t) + u_{m-1,n}(t) + u_{m,n+1}(t)$$
$$+ u_{m,n-1}(t) - 4u_{m,n}(t)] \quad (n > 2). \quad (1)$$

Here $u_{m,n}(t)$ is the displacement, and the equations correspond to $n = 1$, $n = 2$ and $n > 2$, respectively, $\beta = 3$ if $(m, 1)$ belongs to the crack area, where there are no bonds below the row $n = 1$; otherwise, $\beta = 5$. The loading is imposed via a harmonic 'feeding' wave propagating in the same directions as the crack itself. In addition to this wave, there exist reflective (dissipative) waves excited by the propagating crack. In the considered range of the feeding wave frequencies, all these waves are exponentially localized in the vicinity of the interface. In Mishuris et al. (2009), the possibilities are examined for the steady-state regime, where each bond breaks at the same phase of the feeding wave, and for the 'alternating-strain' regime, where the values of the limiting strain alternate in sign. In the present paper, we focus on the steady-state regime.

2.2 The dispersion curves

Consider the complex representation of a localized harmonic wave. In accordance with (1), for the intact lattice

$$u_{m,1} = A_1 \exp[i(\omega t - km)],$$
$$u_{m,2} = u_{m,1}(\beta - 2\cos k - M_1\omega^2/C_1), \quad (2)$$
$$u_{m,n} = u_{m,2}\lambda^{n-2} \quad (n \geq 2, \ \lambda^2 < 1).$$

Recall that for the boundary condition related to the crack area $\beta = 3$; otherwise, $\beta = 5$. The arbitrary coefficient A_1 can be called the complex amplitude of the wave.

We consider two types of the interfaces, with $C_1 = 1$, $M_1 < 1$ and $C_1 > 1$, $M_1 = 1$, with the same ratio C_1/M_1. The dispersion relations, $\omega_1(k)$ and $\omega_2(k)$, and the exponent, λ, follow from (1) and (2). In particular

$$\lambda = \Omega(k) - \sqrt{\Omega^2(k) - 1} \, \text{sign}(\Omega(k)),$$
$$\Omega(k) = 2 - \cos k - \frac{\omega^2}{2} \quad (3)$$

for $\Omega^2 > 1$; in this case, $\lambda^2 < 1$. The dispersion curves and the corresponding exponents λ are shown in Figs. 2, 3, 4, 5, 6 and 7. Note that the dispersion relations correspond to the conditions ahead of the crack front, $\omega = \omega_1(k)$, and to the crack faces, which are traction free, $\omega = \omega_2(k)$.

It can be seen that for a high-contrast interface, Figs. 2 and 3, the waves are strongly localized, and the
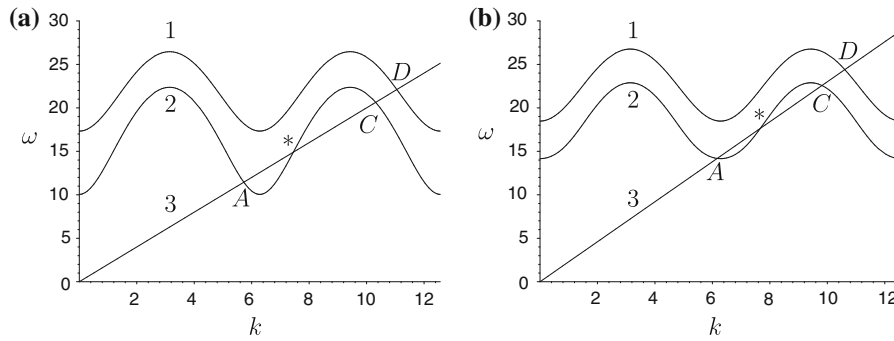
Fig. 2 Dispersion diagrams for $M_1 = 0.01$, $C_1 = 1$ (**a**) and $M_1 = 1$, $C_1 = 100$ (**b**). The *upper* curves (*1*) correspond to the intact lattice, whereas the *lower* ones (*2*) correspond to the traction-free boundary condition. The intersection points of the rays (*3*), $\omega = 2k$ (**a**) and $\omega = 2.3k$ (**b**), with the dispersion curves correspond to the frequencies, ω, and the wavenumbers, k, of the waves with the phase velocity $v = 2$ and $v = 2.3$, respectively.

The condition $v_g = \mathrm{d}\omega/\mathrm{d}k > v$ is satisfied at the intersection point marked by $*$. The other crossings with the curve (*2*) correspond to the reflective (dissipative) waves. The intersection points on the curve (*1*) valid for the crack continuation do not correspond to any wave since $v_g < v$ and hence there is no such a wave ahead of the crack front

Fig. 3 The feeding wave exponents for $M_1 = 0.01$, $C_1 = 1$ (**a**) and for $M_1 = 1$, $C_1 = 100$ (**b**). The *upper* curves (1) correspond to the dispersion curves (*1*), and the *lower* ones (2) correspond to the dispersion curves (2) in Fig. 2
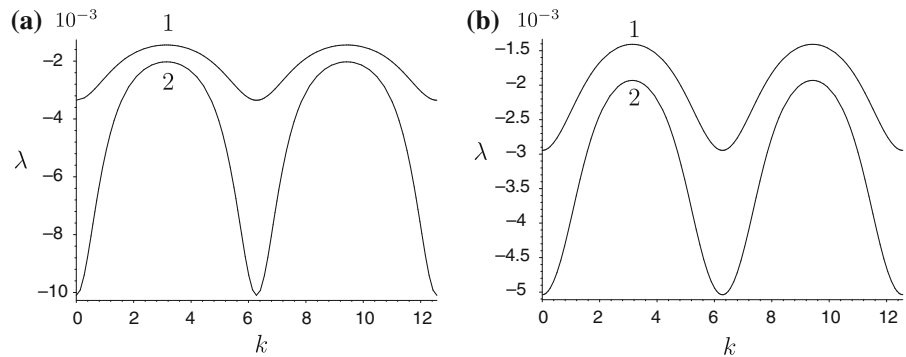
Fig. 4 Dispersion diagrams: **a** $M_1 = 0.1$, $C_1 = 1$, **b** $M_1 = 1$, $C_1 = 10$. The ray (*3*) corresponds to the subsonic phase velocity $v = 0.73$. The other description is similar to that given in the caption to Fig. 2
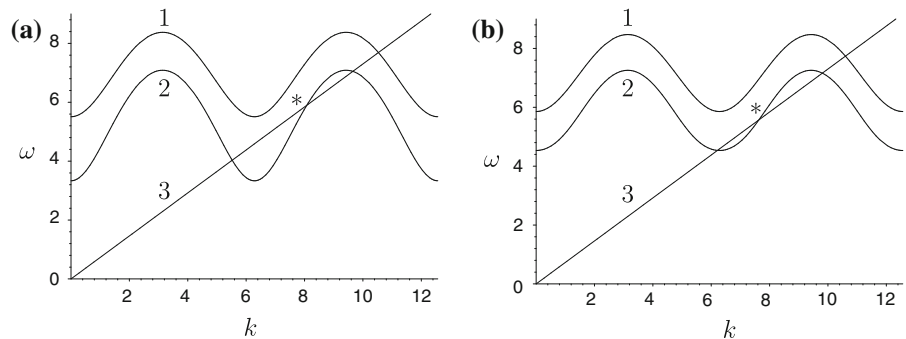

dispersion curves for the cases (a) and (b) are similar. The feeding wave is supersonic relatively to the wave speed in the ambient lattice. The localization, however, takes place in the subsonic case as well.

It follows from (3) that the localized wave can exist if there is a point on the dispersion curve such that at this point

$$\Omega^2 > 1 \implies \omega > \sqrt{2(3 - \cos k)}. \qquad (4)$$

This inequality holds for any k if $\omega > \sqrt{8}$, that is, if the frequency exceeds the upper limit of the harmonic wave frequencies in the ambient lattice. Figures 6 and 7 provide the evidence that such a wave can exist even in the case of a rather low contrast of the interface. In

Fig. 5 The feeding wave exponents for $M_1 = 0.1$, $C_1 = 1$ (**a**) and for $M_1 = 1$, $C_1 = 10$ (**b**). The *upper* curves (*1*) correspond to the dispersion curves (*1*), and the *lower* ones (*2*) correspond to the dispersion curves (*2*) in Fig. 4
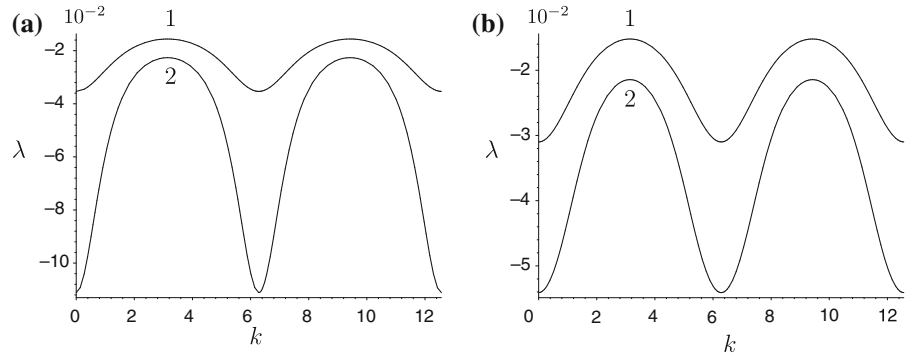
Fig. 6 Dispersion diagrams: **a** $M_1 = 0.4$, $C_1 = 1$, **b** $M_1 = 1$, $C_1 = 2.5$. The ray (*3*) corresponds to the subsonic phase speed $v = 0.35$ (**a**) and $v = 0.38$ (**b**). The other description is similar to that given in the caption to Fig. 2
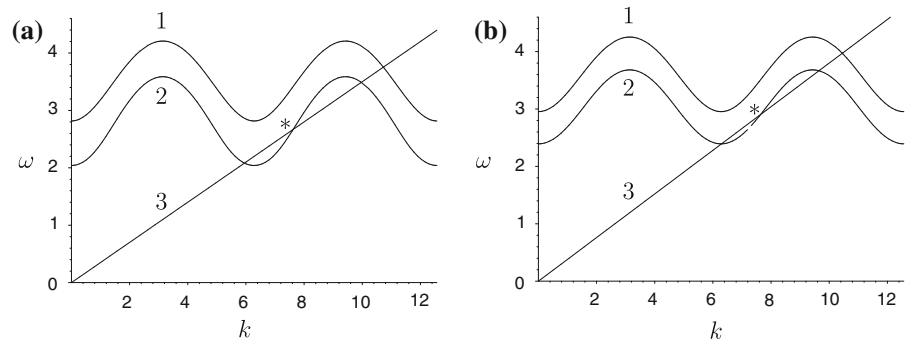
Fig. 7 The feeding wave exponents for $M_1 = 0.4$, $C_1 = 1$ (**a**) and for $M_1 = 1$, $C_1 = 2.5$ (**b**). The *upper* curves (*1*) correspond to the dispersion curves (*1*), and the *lower* ones (*2*) correspond to the dispersion curves (*2*) in Fig. 6
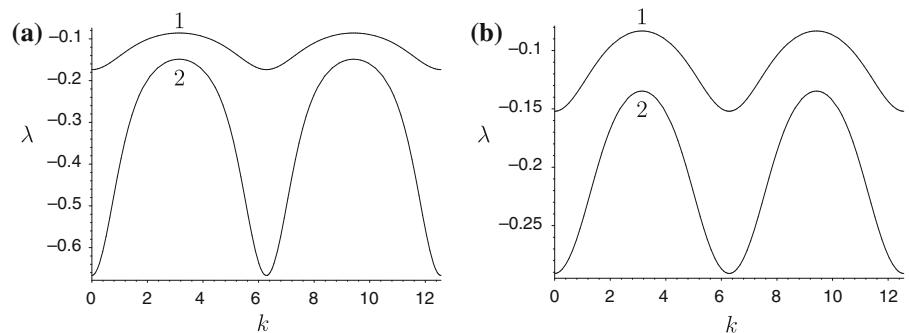
the latter case, however, the radiation from the propagating crack is much more powerful than for the high-contrast interface, but the feeding wave itself remains localized.

The other condition, $v_g > v$, can be satisfied in any case. Indeed, for the discrete lattice the dispersion relation is periodic in k and the phase velocity is not uniquely defined. Thus for a given frequency, which defines the group velocity uniquely, the wavenumber k can always be found in such a way that the inequality is satisfied. We note that the group velocity of the feeding wave must be positive (otherwise, the crack cannot move).

3 Analytical solution for the steady-state regime

The analytical solution is summarized as follows. For the steady-state regime we introduce the variable $\eta = m - vt$ associated with the moving coordinate system. Now $u_{m,n}(t) = U_n(\eta)$. The Fourier transform is used as

$$U_1^F(k) = U_+(k) + U_-(k),$$

$$U_\pm(k) = \pm \int_0^{\pm\infty} U_1(\eta)e^{ik\eta}\,d\eta,$$

$$U_2^F = \int\limits_{-\infty}^{\infty} U_2(\eta) e^{ik\eta} \, d\eta,$$

$$U_n^F(k) = \lambda^{n-2}(k) U_2^F(k) \quad (n \geq 2), \tag{5}$$

where $\lambda(k)$ is defined in (3) with $\omega = 0 + ikv$

$$\lambda^2(k) < 1 \quad (\Omega^2 > 1);$$
$$\lambda = \Omega + i\sqrt{1 - \Omega^2} \, \text{sign} k,$$
$$|\lambda(k)| = 1 \quad (\Omega^2 < 1). \tag{6}$$

Equation (1) for the intact lattice becomes

$$M_1(0 + ikv)^2 U_1^F(k)$$
$$= C_1 \Big[(2\cos k - 5) U_1^F(k) + U_2^F(k) \Big]$$
$$\quad + Q^F(k) \quad (\text{for } n = 1),$$

$$(0 + ikv)^2 U_2^F(k)$$
$$= C_1 \Big[U_1^F(k) - U_2^F(k) \Big]$$
$$\quad + \Big[(2\cos k - 3) U_2^F(k) + U_3^F(k) \Big] \quad (\text{for } n = 2),$$

$$(0 + ikv)^2 U_n^F(k)$$
$$= \Big[(2\cos k - 4) U_n^F(k) + U_{n+1}^F(k)$$
$$\quad + U_{n-1}^F(k) \Big] \quad (\text{for } n > 2), \tag{7}$$

where the body forces, $Q(\eta)$, are introduced to compensate for the action of the broken bonds

$$Q(\eta) = 2C_1 U_1(\eta) H(-\eta), \quad Q^F(k) = 2C_1 U_-(k). \tag{8}$$

This yields the Wiener-Hopf type equation

$$U_+(k) + L(k) U_-(k) = 0 \tag{9}$$

with

$$L(k) = \frac{P_2(k, 0 + ikv)}{P_1(k, 0 + ikv)},$$
$$P_1(k, 0 + ikv) = [M_1(0 + ikv)^2 + C_1(5$$
$$\quad\quad - 2\cos k)] S_2(k, 0 + ikv) - C_1^2,$$
$$P_2(k, 0 + ikv) = [M_1(0 + ikv)^2 + C_1(3$$
$$\quad\quad - 2\cos k)] S_2(k, 0 + ikv) - C_1^2,$$
$$S_2(k, 0 + ikv) = (0 + ikv)^2$$
$$\quad\quad + C_1 + 3 - 2\cos k - \lambda(k), \tag{10}$$

The kernel function of this equation for a periodic lattice of a general structure was analyzed in Slepyan (2002), and it is also straightforward to verify that $L(k)$ has a zero index and $L(k) \to 1$ as $k \to \pm\infty$. This enables us to use the Cauchy type integral to factorize this function, that is, to represent it as a product

$$L(k) = L_+(k) L_-(k), \tag{11}$$

with

$$L_\pm(k) = \exp\left[\pm\frac{1}{2\pi i} \int\limits_{-\infty}^{\infty} \frac{\ln L(\xi)}{\xi - k} \, d\xi \right], \tag{12}$$

where in the latter relation, $\pm \Im k > 0$, respectively.

The factorized form of the equation in (9) is

$$\frac{U_+(k)}{L_+(k)} + L_-(k) U_-(k) = 0. \tag{13}$$

This equation does not have non-trivial solutions corresponding to bounded displacements at $\eta = 0$. To set up a physical problem, with the energy supply to the crack front, we introduce the corresponding Dirac delta function, $\delta(k - k_f)$, as the generalized limit of its analytical representation (see Slepyan 2002, pp. 400–402). Its support, $k = k_f$, is the corresponding zero of $L_+(k)$. The wavenumber $k = k_f$ corresponds to the intersection point marked by $*$ in Figs. 2, 4 and 6. The 'modified' Eq. (13) is

$$\frac{U_+(k)}{L_+(k)} + L_-(k) U_-(k) = A_f \left[\frac{1}{0 + i(k - k_f)} \right.$$
$$\left. + \frac{1}{0 - i(k - k_f)} \right], \tag{14}$$

where A_f is an arbitrary complex constant. In terms of the Fourier transforms, the corresponding solution is

$$U_+(k) = \frac{A_f L_+(k)}{0 - i(k - k_f)},$$
$$U_-(k) = \frac{A_f}{[0 + i(k - k_f)] L_-(k)}. \tag{15}$$

Note that, in addition to the *delta*-function term $A_f \delta(k - k_f)$, the same function but related to the symmetric zero $k = -k_f$ can be introduced as $B_f \delta(k + k_f)$. To get a real solution we take $B_f = \overline{A_f}$. Thus

$$U_+(k) = \frac{A_f L_+(k)}{0 - i(k - k_f)} + \frac{\overline{A_f} L_+(k)}{0 - i(k + k_f)},$$
$$U_-(k) = \frac{A_f}{[0 + i(k - k_f)] L_-(k)}$$
$$\quad + \frac{\overline{A_f}}{[0 + i(k + k_f)] L_-(k)}. \tag{16}$$

For real k

$$U_\pm(-k) = \overline{U_\pm(k)} \tag{17}$$

and hence $U(\eta)$ is indeed a real function.

3.1 The feeding wave

Let the feeding wave amplitude be $|A_1| = A_0$. Referring to (16) we take

$$A_f = \frac{1}{2} A_0 \Phi, \quad \Phi = L_-(k_f) e^{-i\phi}, \qquad (18)$$

where ϕ is an 'initial' phase which defines the position of the wave relative to the breaking bond at the crack front at $\eta = 0$. The feeding wave is defined by the poles $k = \pm k_f$ of the Eq. (16). We obtain

$$U_f(\eta) = A_0 \cos(k_f \eta + \phi) H(-\eta). \qquad (19)$$

Note that there is no such a wave ahead of the crack front.

3.2 The dissipative waves

The dissipative waves are related to the other two intersection points on the dispersion curves 2 in Figs. 2, 4 and 6. Let us denote the corresponding wavenumbers by k_A and k_C (see Fig. 2). We also introduce the quantities

$$L_-^*(k_A) = \lim_{k \to k_A} \frac{L_-(k)}{0 + i(k - k_A)},$$
$$L_-^*(k_C) = \lim_{k \to k_C} \frac{L_-(k)}{0 + i(k - k_C)}. \qquad (20)$$

It follows that the dissipative waves amplitudes are

$$W = 2A_0 \frac{\sqrt{k_0^2 (\Re\Phi)^2 + k_f^2 (\Im\Phi)^2}}{|k_0^2 - k_f^2||L_-^*(k_0)|}. \qquad (21)$$

Here $k_0 = k_A$ and $k_0 = k_C$ for k_A and k_C-waves, respectively. These waves propagate behind the crack front. There are no waves propagating ahead of the crack.

3.3 Contribution of the pole at $k = 0$

It can be found that the pole at $k = 0$ yields a constant displacement at $\eta < 0$

$$U_0(\eta) = -\frac{A_0}{k_f L_-^0(0)} \Im\Phi, \quad L_-^0(0) = \lim_{k \to 0} \frac{L_-(k)}{0 + ik}. \quad (22)$$

Note that $L_-^0(0) > 0$. Thus, in addition to the oscillations defined by the feeding and dissipative waves, there is a relative shift of the crack faces caused by the oscillating waves (in fact, it tends to a constant as
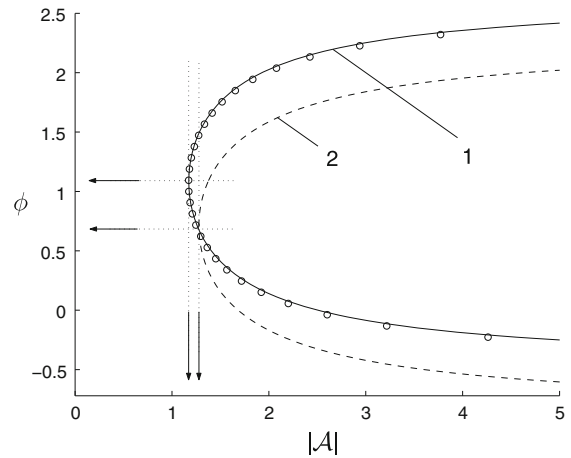
Fig. 8 The normalized amplitude of the feeding wave, $\mathcal{A}$, versus 'initial phase' ϕ. For the two-dimensional lattice two cases are shown: $M_1 = 0.01$, $v = 2$ with $\mathcal{A}_{min} = 1.174$ ($\phi = 1.0849$) (_1_), and $M_1 = 0.05$, $v = 1.05$ with $\mathcal{A}_{min} = 1.278$ ($\phi_2^{min} = 0.7076$) (_2_). The _circles_ correspond to the lattice strip, $M = 1$, $v = 0.2$

$\eta \to -\infty$). This is the illustration of the phenomenon known as a drift of a finite mass or a shift of an infinite elastic structure under a harmonic load. The drift speed, as well as the shift, depends on the phase of the load at the instant time when it is applied.

3.4 The wave amplitude and the initial phase

The strain energy of the broken bond is

$$G_0 = U^2(0), \qquad (23)$$

where the total displacement at the moment of the bond breakage can be obtained from (16) and (18) as a limit

$$U(0) = \lim_{s \to \infty} sU_+(is) = \lim_{s \to \infty} sU_-(-is) = A_0 \Re\Phi. \qquad (24)$$

Now, using the fracture criterion, we get

$$\Re\Phi = \Re\left[L_-(k_f) e^{-i\phi}\right] = \frac{u_c}{A_0}. \qquad (25)$$

Given the feeding wave amplitude, A_0, and the critical elongation u_c, this relation can be used for the determination of the phase ϕ. On the contrary, we can fix ϕ and determine the relations between the amplitudes of the feeding and dissipative waves and the critical elongation of the bond. Some relations between the normalized amplitude, $\mathcal{A} = A_0/u_c$, and the phase, ϕ, are presented in Fig. 8.

4 Energy relations

4.1 General dependencies

For a localized sinusoidal wave (2) the energy flux, N, is defined as the product of the force acting on a particle from the left, and its velocity. From (2) it can be found that the energy flux in the wave propagating in the crack area is

$$N = \frac{1}{2}|A_1|^2 kv \sin k$$
$$\times \left[C_1 + \frac{(3 - 2\cos k - M_1\omega^2/C_1)^2}{1 - \lambda^2(k)} \right], \quad (26)$$

where A_1 is the complex wave amplitude, k is the wave number, $\lambda(k)$ is the corresponding exponent and v is the phase velocity. Note that if $C_1 = 1$ then Eq. (26) is simplified

$$N = \frac{1}{2} \frac{|A_1|^2 kv \sin k}{1 - \lambda^2(k)}. \quad (27)$$

The energy per unit length of the crack front advance, corresponding to a wave with parameters k, λ and $v_g = \mathrm{d}\omega/\mathrm{d}k$, is

$$G = \frac{N}{vv_g}|v_g - v|. \quad (28)$$

In particular, for the feeding wave $G = G_f$ is the energy carried to the crack front, whereas for a localized dissipative wave this is the energy radiated from the crack front. We denote the dissipative waves energies corresponding to the intersection points A and C, marked in Fig. 2, by G_A and G_C, respectively. Note that the group velocity can be positive, zero or negative, but, in the considered structures, the ratio $(\sin k)/v_g$ is always positive and bounded.

4.2 The energy radiated from the interface

We consider the energy flux from the nod (m, n) to the nod $(m, n + 1)$. Due to the periodicity, the choice of the value of m is not important. The total energy transfer is

$$G_{n\to n+1} = \int_{-\infty}^{\infty} [u_{m,n}(t) - u_{m,n+1}(t)]\dot{u}_{m,n+1}(t)\,\mathrm{d}t. \quad (29)$$

Using the Parseval identity and taking into account the fact that

$$U_{n+1}^F(k) = U_n^F(k)\lambda(k) = U_2^F(k)\lambda^{n-1}(k) \quad (n \geq 2) \quad (30)$$

we can express this in the form

$$G_{n\to n+1} = -\int_{-\infty}^{\infty} [U_n(\eta) - U_{n+1}(\eta)]\frac{\mathrm{d}U_{n+1}(\eta)}{\mathrm{d}\eta}\,\mathrm{d}\eta$$
$$= -\frac{1}{2\pi} \int_{-\infty}^{\infty} \left[U_n^F(k) - U_{n+1}^F(k) \right]$$
$$\times \overline{(-ik)U_{n+1}^F(k)}\,\mathrm{d}k$$
$$= -\frac{1}{2\pi} \int_{-\infty}^{\infty} |U_2^F(k)|^2$$
$$\times [1 - \lambda(k)]|\lambda|^{n-2}\overline{(-ik)\lambda(k)}\,\mathrm{d}k. \quad (31)$$

In accordance with (7) we have

$$U_2^F(k) = \left(5 - 2\cos k - \frac{M_1}{C_1}k^2v^2 \right) U_+(k)$$
$$+ \left(3 - 2\cos k - \frac{M_1}{C_1}k^2v^2 \right) U_-(k). \quad (32)$$

In the integral (31), only the imaginary part of $\lambda(k)$ gives a contribution. In the corresponding domain, $|\lambda(k)| = 1$ and the integral becomes

$$G_{n\to n+1} = G_r = \frac{1}{\pi} \int_{\mathcal{K}} |U_2^F(k)|^2 \sqrt{1 - \Omega^2}\,k\,\mathrm{d}k. \quad (33)$$

The domain $\mathcal{K}$ is that in the positive half-axis $k > 0$, where $\Omega^2 < 1$. In particular, if the latter inequality is valid and $C_1 = 1$, then $|U_2^F(k)| = |U_1^F(k)|$. The energies of the waves as functions of ϕ are plotted in Figs. 9, 10 and 11.

5 Crack-speed oscillation regimes

5.1 The lattice strip

Since, in the above-considered example for a high-contrast interface, the exponent $|\lambda| \ll 1$, a good approximation can be achieved by means of a one-dimensional model. In Mishuris et al. (2009) such a model was used for the numerical simulations. A chain was considered as the interface layer with the line $n = 2$ fixed. This model is an asymptotic one for large
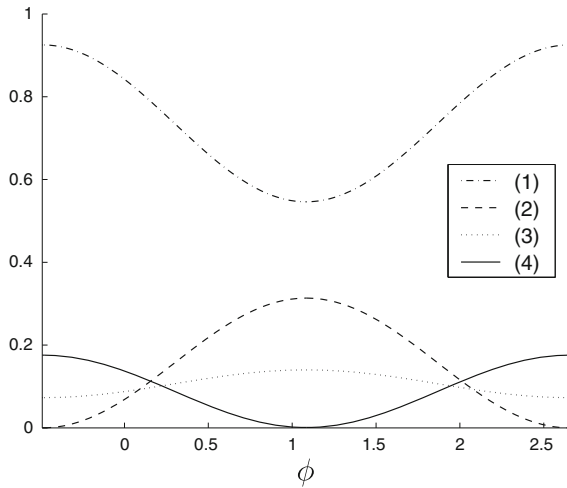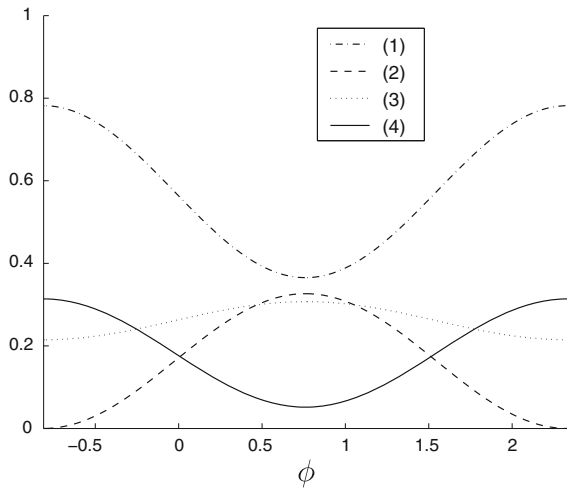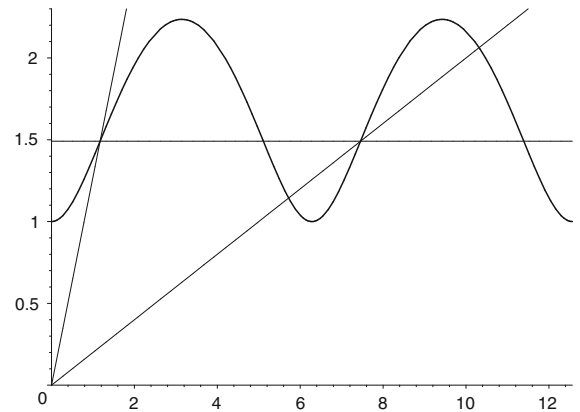
Fig. 9 Normalized energies for the case $M_1 = 0.01, C_1 = 1$: G_a/G_f (*1*), G_0/G_f (*2*), G_c/G_f (*3*), $10^2 \cdot G_r/G_f$ (*4*)
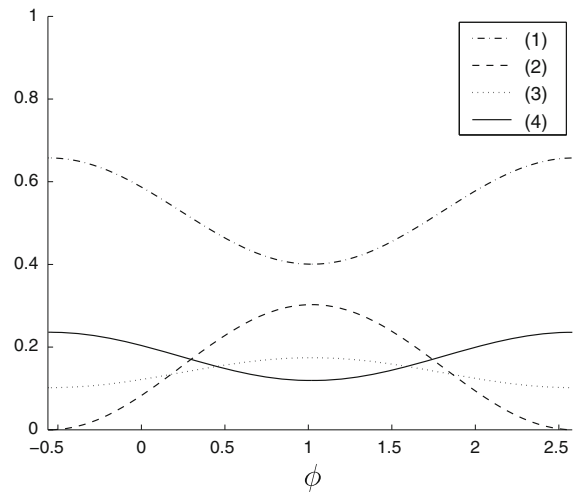
Fig. 11 Normalized energies for the case $M_1 = 0.4, C_1 = 1$: G_a/G_f (*1*), G_0/G_f (*2*), G_c/G_f (*3*), G_r/G_f (*4*)

Fig. 10 Normalized energies for the case $M_1 = 0.1, C_1 = 1$: G_a/G_f (*1*), G_0/G_f (*2*), G_c/G_f (*3*), $10^2 \cdot G_r/G_f$ (*4*)

Fig. 12 The dispersion curve $\omega_2(k)$ for the strip and the rays $\omega = 0.2k$ and $\omega = 1.272k$

ratio M_2/M_1. The chain was assumed to consist of the unit masses $m = 0, 1, \ldots, m_{end} = 200$ with the initial crack at $m = 0, 1, \ldots, m_*(0) = 51$. The bond stiffness was taken as a natural unit too. The system of ordinary differential equations under zero initial conditions was considered as

$$u_0 = A \sin(\omega_f t) H(t), \quad u_{m_{end}} = 0,$$
$$\ddot{u}_m = -3u_m + u_{m-1} + u_{m+1} \quad (m < m_*(t)),$$
$$\ddot{u}_m = -5u_m + u_{m-1} + u_{m+1} \quad (m \geq m_*(t)), \qquad (34)$$

where $m_*(t)$ is the crack front. At the moment when u_m first reaches the critical value, the corresponding bond (below the mass) breaks and m_* gains a unit increment.

For such a lattice strip

$$\omega = \omega_1(k) = \sqrt{5 - 2\cos k} \quad \text{for the intact chain,}$$
$$\omega = \omega_2(k) = \sqrt{3 - 2\cos k} \quad \text{for the crack region.} \quad (35)$$

With the reference to the above-considered high-contrast case $M_1 = 0.01, v = 2$ we have taken $\omega_f = 1.491 (k_f = 7.455)$, and the numerical simulations were expected to result in the steady-state regime (at least for a moderate amplitude $\mathcal{A}$) with $v = 0.2, v_g = 0.618$. The dispersion dependence $\omega_2(k)$ is plotted in Fig. 12.

Fig. 13 The cluster-averaged crack speed as a function of the feeding wave amplitude. **a** $\mathcal{A}^* < \mathcal{A} < 10$, **b** $\mathcal{A}^* < \mathcal{A} < 100$
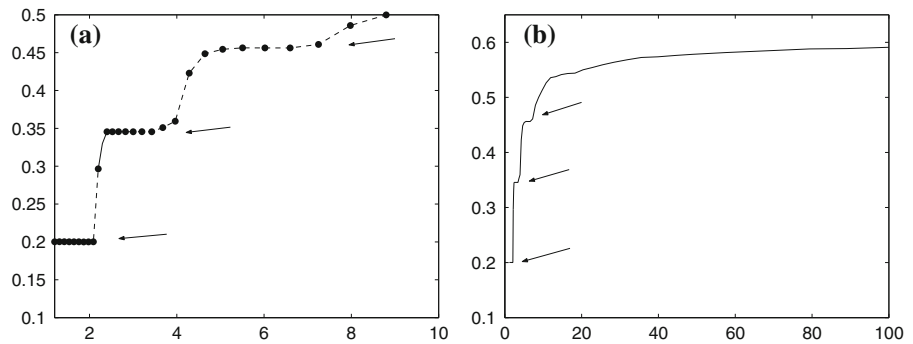
5.2 Crack speeds in numerical simulations

The problem corresponding to the high-contrast interface of the lattice was analyzed in Mishuris et al. (2009) numerically. Two formulations of the fracture criterion were used: the steady-state formulation: $u_m = u_c > 0$, and the alternate-strain formulation: $|u_m| = u_c > 0$. Here we address the steady-state formulation.

Figure 13 gives the numerically obtained average crack speed as a function of the normalized feeding wave amplitude $\mathcal{A} = A/u_c$. If $\mathcal{A} < \mathcal{A}^* = 1.177$, the crack growth, even if initiated, stops. As $\mathcal{A} > \mathcal{A}^*$ the crack propagates, and the crack speed is independent of the amplitude within the interval $\mathcal{A} \in (\mathcal{A}^*, 2.18]$; this crack speed is equal to the theoretically predicted speed $v = v_{\text{steady}} = 0.2$. On the other hand, further increase in the amplitude results in the increase of the average crack speed, which approaches the value of the feeding wave group velocity $v_g = 0.618$ as '$\mathcal{A} \to \infty$'.

In Fig. 14 the position of the crack front is shown as a function of time for different amplitudes of the feeding wave. In particular, for the two chosen values, $\mathcal{A} = 1.2$ and 2.0, the speeds of the crack are the same, and the time-interval between the breakage of the neighboring bonds is constant, equal to $1/v$ that corresponds to the steady-state regime. At the higher values of the amplitude, the average speed is established within an interval as $\mathcal{A}$-dependent constant, whereas the local crack speed is non-uniform; it oscillates between the steady-state value, $v = 0.2$, and a higher value. This non-uniformity in the local crack speed is shown in more detail in Fig. 15. It can be seen that at a very large amplitude multiple local speeds arise; however, even in such a locally disordered crack growth, the average crack speed is established on a macro-level scale; it is shown to be a function of the amplitude only.
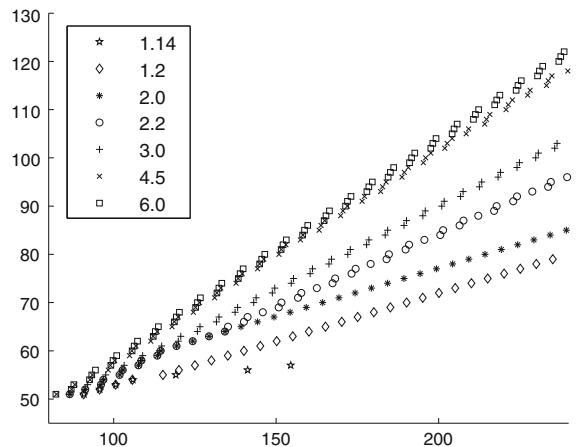
Fig. 14 Positions of the crack front at the moment of the bond breakage versus time. The values of the amplitude, $\mathcal{A}$, are listed in the insert. The steady-state regime is established with $v = 0.2$ for $\mathcal{A} = 1.2$ and $\mathcal{A} = 2.0$. The oscillating crack speed regime is established with the increased average speeds for $\mathcal{A} = 2.2, \ldots, 6.0$

5.3 Cluster-type wave representation

Consider a chain of particles, of unit mass, numbered by $m = 0, \pm 1, \pm 2, \ldots$. Assume that neighboring particles are connected with each other by bonds of unit stiffness, and, in addition, each particle is connected with a rigid base by a bond of the stiffness C. The bonds are assumed to be massless and linearly elastic. Note that, in the above considered crack problem, $C = 1$ behind the crack front, and $C = 3$ at the front and ahead of it (see Fig. 1 where the line $n = 2$ is fixed). The dynamic equation is

$$\frac{d^2 u(t, m)}{dt^2} + (2 + C)u(t, m) - u(t, m + 1) - u(t, m - 1) = 0, \tag{36}$$

Fig. 15 The intervals between the breakage of the neighboring bonds versus the sequence of the breakages of the bonds
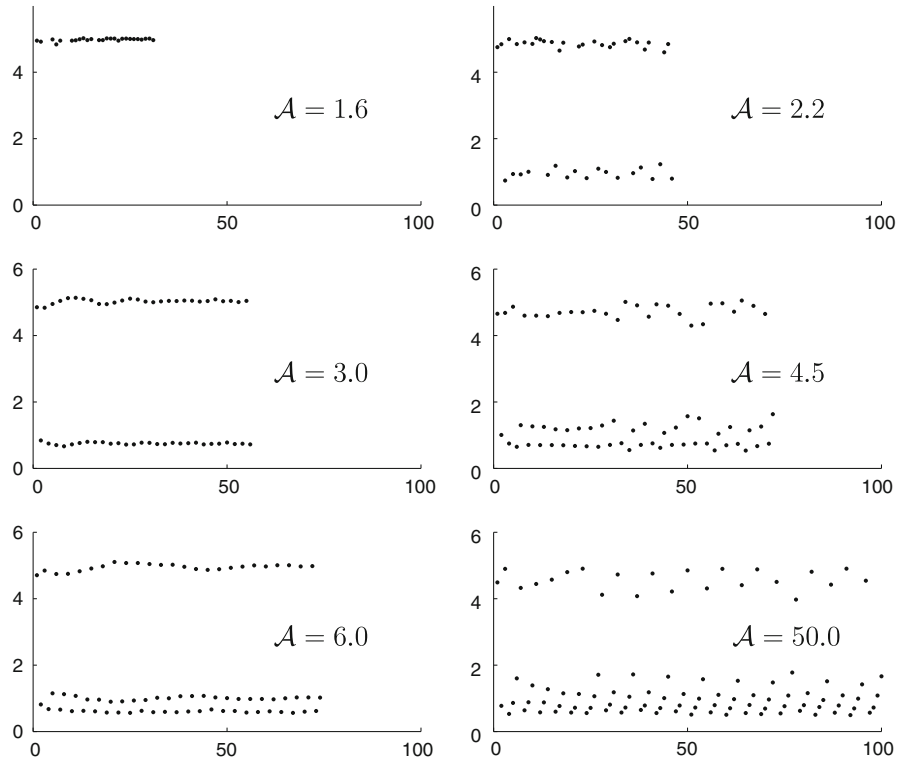
where u is the displacement. The primitive solution to this equation for $C = \text{const}$ is a harmonic wave

$$u(t, m) = e^{i(\omega t - km)}, \qquad (37)$$

where the frequency ω is coupled with the wavenumber k by dispersion relation

$$\omega^2 = C + 2(1 - \cos k). \qquad (38)$$

Given the frequency, in such a discrete system, the wavenumber is not defined uniquely, namely, if $k = k^0$, $-\pi < k^0 \le \pi$, satisfies (38) then any $k = k_n = k^0 + 2\pi n$, $n = 0, \pm 1, \ldots$, also satisfies this relation. This non-uniqueness, however, does not affect the particles motion since it does not affect the wave (37) at the integer m, and the group velocity (which is equal to the energy flux velocity)

$$v_{\text{g}} = \frac{d\omega}{dk} = \frac{\sin k}{\omega} \qquad (39)$$

is defined uniquely. The only characteristic of the wave, which depends on the choice of k, is the phase speed

$$v = \frac{\omega}{k}. \qquad (40)$$

For such a system, where $m = 0, \pm 1, \ldots$, it is usually assumed that $k = k^0$. Otherwise, during the time-period $1/v$, when a fixed phase moves from one particle to the other, this phase appears at the latter

n times. Nevertheless, as we show below, the phase speed non-uniqueness, $v = v_n = \omega/k_n$, is useful in the analysis of the steady-state and the cluster-type regimes of the crack motion under the sinusoidal wave.

The characteristic feature of the wave (37) is the periodicity

$$u(t, m + 1) = u(t - 1/v, m). \qquad (41)$$

The phase speed places an important role in the interaction of the wave with a moving obstacle, in particular, with an advancing crack. In the established, 'steady-state' regime, the crack speed is equal to the phase speed of the wave, that is, the lattice bonds along the crack path break in equal time-intervals and at the same phase of the 'feeding wave' which forces the crack to grow. In this case, the periodicity relation (41) is valid for the lattice-with-crack displacements. For a given value of the frequency (within the passing band), if there are no other restrictions, the allowed set of the crack speeds is $v = \omega/(k^0 \pm 2\pi n)$, where n is any integer.

Recall that the real crack speed must be below the group velocity of the feeding wave. Otherwise, the wave cannot deliver energy to the moving crack front. Thus, in the above-shown results of the numerical

simulations, the steady-state crack speed, equal to the phase speed of the feeding wave, is equal to $\omega/(k^0 + 2\pi)$. This is because the 'main' value, $v = \omega/k^0$, corresponds to the opposite inequality, $\omega/k^0 > v_{\mathrm{g}}$, and hence cannot be realized. Note, however, that at lager amplitudes, where the crack-speed oscillating regimes are realized, the group velocity is required to be greater than the average crack speed; some of the local speeds can exceed the group velocity.

In the latter case, the average crack speed can be approximated by a piece-wise constant function of the amplitude of the feeding wave. Each interval of the amplitude corresponding to a plateau of the average crack speed is characterized by a period of the crack-speed oscillations. At a discrete set of threshold values of the feeding wave amplitude, the number of lattice particles in the cluster, which the crack front passes during the period, gains a unit increment and the average crack speed increases. This suggests the viability of a cluster-type wave representation.

We now construct a wave corresponding to several particles in the cell of periodicity. The uniformity of the structure allows us to take the cell of any width; let it consist of $n \geq 1$ particles. We mark the particles within the cell by the subscript $q = 0, 1, 2, \ldots, n - 1$, and introduce a composite wave, U, consisting of n 'sinusoidal waves'

$$U(t, m) = \sum_{q=0}^{n-1} u_q \exp[\mathrm{i}(\omega t - km_q)]\delta_{m,m_q},$$
$$m_q = q, \, q \pm n, \, q \pm 2n, \ldots, \tag{42}$$

where δ_{m,m_q} is the Kronecker delta. Eq. (36) yields the system

$$Su_0 - \mathrm{e}^{-\mathrm{i}k}u_1 - \mathrm{e}^{\mathrm{i}k}u_{n-1} = 0,$$
$$-\mathrm{e}^{\mathrm{i}k}u_0 + Su_1 - \mathrm{e}^{-\mathrm{i}k}u_2 = 0,$$
$$-\mathrm{e}^{\mathrm{i}k}u_1 + Su_2 - \mathrm{e}^{-\mathrm{i}k}u_3 = 0,$$
$$- - - - - - - - - - - -,$$
$$-\mathrm{e}^{-\mathrm{i}k}u_0 - \mathrm{e}^{\mathrm{i}k}u_{n-2} + Su_{n-1} = 0, \tag{43}$$

where $S = 2 + C - \omega^2$. There are n eigen-solutions which satisfy this system

$$u_{q+1} = u_q \mathrm{e}^{2\pi \mathrm{i}p/n}, \quad p = 0, 1, \ldots, n - 1, \tag{44}$$

with

$$\omega^2 = C + 2 - 2\cos(k - 2\pi p/n). \tag{45}$$

Note that this dispersion relations differ only by a shift along the k-axis. Thus, the waves are

$$u_q \exp[\mathrm{i}(\omega t - km_q)] = u_0 \exp[\mathrm{i}(\omega t - km_q + 2\pi qp/n)]$$
$$= u_0 \exp[\mathrm{i}(\omega t - k_0 m)],$$
$$k_0(\omega) = k - 2\pi p/n, \tag{46}$$

where k_0 is, in fact, independent of n, p and q. Thus the group velocity depends on the frequency only

$$v_{\mathrm{g}} = \frac{\mathrm{d}\omega}{\mathrm{d}k} = \frac{\sin[k_0(\omega)]}{\omega}, \tag{47}$$

Furthermore, since the dispersion relation (45) is independent of q, for any given n and p the phase speeds of the waves in (42) are also the same. The periodicity relation valid for the cluster and the cluster-associated phase speed are

$$U(t, m + 1) = U(t - n/v, m),$$
$$v = v_n = \frac{\omega}{k} = \frac{\omega}{k_0 - 2\pi(p - 1)/n}. \tag{48}$$

The average crack speed, however, must be below the feeding wave group velocity $v_{\mathrm{g}} = \mathrm{d}\omega/\mathrm{d}k$ which, in contrast to the phase speed, is uniquely defined.

Thus the admissible average crack speeds are

$n \backslash p$	1	2	3	4	5	6
1	**0.2**					
2	0.2	**0.3457**				
3	0.2	0.2781	**0.4565**			
4	0.2	0.2534	0.3457	**0.5436**		
5	0.2	0.2405	0.3017	0.4046	**0.6140**	
6	0.2	0.2327	0.2781	0.3457	0.4565	(0.6719)

where the speed shown in brackets cannot be realized because it exceeds the group velocity.

The maximal speeds shown in bold correspond to those obtained in the numerical simulations (compare the first four values, **0.2**, …, **0.5436**, with the 'plateau speeds' shown in Fig. 13a, b).

Now we discuss Fig. 15 and pay attention to the time intervals corresponding to the wave amplitude $\mathcal{A} = 3$. The upper line value is approximately equal to 5 that meets the steady-state speed, while the lower line value is approximately equal to 0.8. In this respect, we note that the feeding wave frequency $\omega \approx 1.491$, and the 'main' phase speed $v_0 = \omega/(k_f - 2\pi) \approx 1.272$ ($k_f > \pi$, $0 < k_f - 2\pi < \pi$). Recall that it is greater than the group velocity $v_{\mathrm{g}} \approx 0.618$, and hence the steady-state regime with this speed is impossible. However, in the crack-speed oscillation regime this restriction concerns only with the average crack speed, and the local speed can be increased. It can be seen that the

time interval corresponding the main phase speed is just $1/1.272 \approx 0.786$ that is in a good agreement with the lower lane. Thus, at this amplitude, the local crack speeds alternate: they are equal to the main and to the second values of the feeding wave phase speed.

6 Flexural plate as a continuous model

The elastic flexural plate is an example where the steady-state crack growth can occur under a harmonic wave as well as in the lattice. The necessary conditions remain the same: the wave radiated by a remote source must be localized, and its group velocity must exceed the phase one, and these conditions are satisfied in the case of a flexural plate. The approach is similar to that used for the lattice. The main difference lies in the dispersion curves which now are not periodic, the frequency monotonically increases as the wavenumber grows. The latter gives no direct evidence respective to possible crack-speed oscillation regime.

6.1 The model

The classical dynamic equation for the elastic flexural plate is

$$\Delta^2 w(x, y, t) + \frac{\partial^2 w(x, y, t)}{\partial t^2} = 0,$$
$$\Delta = \frac{\partial^2}{\partial x^2} + \frac{\partial^2}{\partial y^2}, \qquad (49)$$

where w is the transversal displacement. The bending moments and transversal forces are expressed as follows:

$$M_y = -\left(\frac{\partial^2 w}{\partial y^2} + v \frac{\partial^2 w}{\partial x^2} \right),$$
$$Q_y = -\frac{\partial}{\partial y} \left(\frac{\partial^2 w}{\partial y^2} + (2 - v) \frac{\partial^2 w}{\partial x^2} \right),$$
$$M_x = -\left(\frac{\partial^2 w}{\partial x^2} + v \frac{\partial^2 w}{\partial y^2} \right),$$
$$Q_x = -\frac{\partial}{\partial x} \left(\frac{\partial^2 w}{\partial x^2} + (2 - v) \frac{\partial^2 w}{\partial y^2} \right). \qquad (50)$$

Here, we use the natural units: h (length), $h\sqrt{12(1-v^2)\varrho/E}$ (time) and $Eh^2/[12(1-v^2)]$ (force), where E, v, ϱ and h are the elastic modulus, Poisson's ratio, density and the plate thickness, respectively.

It is assumed that there exists a semi-infinite transverse crack growing in the x-direction at $y = 0$. As in the case of the lattice we first consider waves corresponding to the conditions on the free crack faces and to the crack continuation.

6.2 The waves

We use the representation

$$w = \exp[-\lambda y + i(\omega t - kx)]. \qquad (51)$$

Four values of λ follow from (49)

$$\lambda = \lambda_{1,2} = \sqrt{k^2 \pm \omega} \quad \text{and} \quad \lambda = \lambda_{3,4} = -\sqrt{k^2 \pm \omega}. \qquad (52)$$

6.3 Symmetric problem

Consider the upper half-plane, $y > 0$, with two types of the boundary conditions at $y = 0$ related to the crack problem

$$\frac{\partial w}{\partial y} = Q_y = 0 \ (a) \quad \text{and} \quad M_y = Q_y = 0 \ (b). \qquad (53)$$

These conditions yield the dispersion relations as

$$\omega = \pm k^2 \ (a) \quad \text{and} \quad \omega = \pm \alpha k^2 \ (b), \qquad (54)$$

where $\alpha = \alpha(v) < 1$ $(v > 0)$ is the positive root of the equation

$$(1 - v + \alpha)^2 \sqrt{1 - \alpha} - (1 - v - \alpha)^2 \sqrt{1 + \alpha} = 0. \qquad (55)$$

Note that α monotonically tends to 1 as $v \to 0$; $\alpha \approx 0.9783$ for $v = 1/2$. The relations (a) correspond to an y-independent flexural wave (51) with $\lambda = 0$

$$w = \exp[i(\omega t - kx)], \qquad (56)$$

and the relation (b) corresponds to an edge wave exponentially decreasing with the distance from the free boundary of the plate. It can be represented as

$$w = A_0 \left[\exp\left(-\sqrt{1 + \alpha}\, |k|\, y \right) \right.$$
$$\left. - \frac{1 - v + \alpha}{1 - v - \alpha} \exp\left(-\sqrt{1 - \alpha}\, |k|\, y \right) \right]$$
$$\times \exp[i(\omega t - kx)]. \qquad (57)$$

Note that the latter and the corresponding relation for the case of the plate-fluid interaction were presented in Slepyan (2002, p. 349–351).

For both waves, the group velocity $v_g = d\omega/dk$ is greater than the phase velocity, $v = \omega/k$, $v_g = 2v$. Given the feeding wave frequency, the crack speed is defined by the the dispersion relation (b) in (54).

The dynamic crack growth in the flexural plate is accompanied by the wave radiation. It is shown below that the waves radiated from the moving crack front correspond to the dispersion relation (a) in (54), that is, to the point $k = \pm\omega$ which correspond to the wave propagating in the x-direction, and to the region $-\sqrt{\omega} < k < \sqrt{\omega}$ which corresponds to waves radiated at angle of this axis.

6.4 The crack problem

We now consider the plate with a crack propagating along the x-axis with a constant speed, v, and introduce the steady-state problem variable $\eta = x - vt$: $w = w(\eta, y)$. The crack area is at the left, $\eta < 0$, where we do not take into account possible crack closure effect. The conditions at $y = +0$ are

$$M_y = Q_y = 0 \ (\eta < 0), \quad \frac{\partial w}{\partial y} = Q_y = 0 \ (\eta > 0). \tag{58}$$

Using the Fourier transform on η

$$f^F(k, y) = f_+ + f_-,$$
$$f_\pm = \pm \int_0^{\pm\infty} f(\eta, y) \exp(ik\eta) \, d\eta, \tag{59}$$

the causality principle for the steady-state formulation (see Slepyan 2002, pp. 91–93) and the condition $Q_y = 0$ at $y = 0$ we find

$$w^F(k, y) = A \exp(-\mu_1 y) - B \exp(-\mu_2 y),$$
$$B = A \frac{\mu_1 (\mu_2^2 - vk^2)}{\mu_2 (\mu_1^2 - vk^2)},$$
$$\mu_{1,2} = \sqrt{k^2 \pm (kv - i0)}. \tag{60}$$

Now, comparing the expressions for $M_y^F(k, 0) = M_+(k)$ and $\partial w^F(k, 0)/\partial y = \psi_-(k)$ we obtain the Wiener-Hopf equation

$$M_+(k) - L(k)\psi_-(k) = 0 \tag{61}$$

with

$$L(k) = \frac{\mu_2 (\mu_1^2 - vk^2)^2 - \mu_1 (\mu_2^2 - vk^2)^2}{2\mu_1\mu_2(kv - i0)}. \tag{62}$$

The following features of the kernel $L(k)$ are important:

$$\Re L(-k) = \Re L(k), \ \Im L(-k) = -\Im L(k), \ \mathrm{Ind}L(k) = 0,$$
$$L(k) = \frac{(1 - \nu)(3 + \nu)}{2}|k| + O\left(\frac{1}{k}\right) \ (k \to \pm\infty),$$
$$L(k) \sim \frac{1 + i}{2}\sqrt{kv - i0} \ (k \to 0), \tag{63}$$

and $\Im L(k)$ has a finite support. Note that $k = \pm k_f - i0$ are the zeros of the numerator of $L(k)$ [compare (62) and (55)]. It is convenient to normalize this function; we represent it as follows:

$$L(k) = L^0(k)l(k),$$
$$l(k) = \frac{(1 - \nu)(3 + \nu)}{2}$$
$$\times \frac{[0 - i(k - k_f)][0 - i(k + k_f)]\sqrt{0 + ik}}{\sqrt{(0 - ik)[0 - i(k - v)][0 - i(k + v)]}},$$
$$\left[L^0(k) \to 1 \ (k \to \pm\infty), \quad \mathrm{Ind}L^0(k) = 0 \right]. \tag{64}$$

Next step is the factorization

$$L(k) = L_+(k)L_-(k), \quad L_+ = L_+^0 l_+, \quad L_- = L_-^0 l_-, \tag{65}$$

where the functions $L_\pm^0(k)$ are defined by the Cauchy type integral

$$L_\pm^0(k) = \exp\left[\pm\frac{1}{2\pi i} \int_{-\infty}^{\infty} \frac{\ln|L^0(\xi)| + i\mathrm{Arg}L^0(\xi)}{\xi - k} \, d\xi \right]. \tag{66}$$

In the integrand, $\Im k > 0$ for $L_+(k)$, $\Im k < 0$ for $L_-(k)$, and $\mathrm{Arg}L^0(\xi) = 0$ for $|\xi| > v$. In turn

$$l_+(k) = \sqrt{\frac{(1 - \nu)(3 + \nu)}{2}}$$
$$\times \frac{[0 - i(k - k_f)][0 - i(k + k_f)]}{\sqrt{(0 - ik)[0 - i(k - v)][0 - i(k + v)]}},$$
$$l_-(k) = \sqrt{\frac{(1 - \nu)(3 + \nu)}{2}}\sqrt{0 + ik}. \tag{67}$$

In particular, it follows from (66) that asymptotes of the factors $L_\pm(k)$ are

$$L_\pm(k) \sim \sqrt{\frac{(1 - \nu)(3 + \nu)}{2}}\sqrt{0 \mp ik} \ (k \to \pm i\infty). \tag{68}$$

The equation in (61) can now be rearranged in the form

$$\frac{M_+(k)}{L_+(k)} - L_-(k)\psi_-(k) = \frac{A}{0 + \mathrm{i}(k - k_f)}$$
$$+ \frac{A}{0 - \mathrm{i}(k - k_f)}, \qquad (69)$$

where the right-hand side includes the analytical representation of the delta-function which corresponds to the localized feeding wave (in this connection, see Slepyan 2002, pp. 400–403). Its wavenumber k_f is defined in (54): $k_f = \sqrt{\omega/\alpha} = v/\alpha$. Note that we keep in mind that such a function is also introduced at $k = -k_f$ as $\overline{A}\left[1/(0 + i(k + k_f)) + 1/(0 - i(k + k_f))\right]$, and this makes $M(\eta)$ and $\psi(\eta)$ to be real functions. Thus, we can consider real parts of the functions, as obtained directly from (69)

$$M_+(k) = \frac{AL_+(k)}{0 - \mathrm{i}(k - k_f)},$$
$$\psi_-(k) = -\frac{A}{[0 + \mathrm{i}(k - k_f)]L_-(k)}. \qquad (70)$$

The feeding wave is reflected by the function $\psi(\eta)$ ($\eta \to -\infty$, $y = +0$), which is defined by the residue at $k = k_f$ of the corresponding expression in (70) as

$$\psi(\eta) = \frac{\partial w(\eta, 0)}{\partial y} = -\frac{A}{L_-(k_f)} \exp[\mathrm{i}(\omega t - k_f x)],$$
$$\omega = k_f v. \qquad (71)$$

Comparing this with the expression for $\partial w(\eta, 0)/\partial y$ following from (57) we find the coefficient A_0 and the complex amplitude of the feeding wave $\mathcal{A}$ [see (55)]

$$A_0 = A \frac{1 - \nu - \alpha}{2\alpha k_f L_-(k_f)}(1 - \alpha^2)^{-1/4},$$
$$\mathcal{A} = -A_0 \frac{2\alpha}{1 - \nu - \alpha}$$
$$= -\frac{A}{k_f L_-(k_f)}(1 - \alpha^2)^{-1/4}. \qquad (72)$$

The energy delivered by the feeding wave per unit area of the crack path is

$$G = \frac{1}{v} \int_0^\infty \Re \left[\overline{M_x}(\eta, y) \frac{\partial^2 w(\eta, y)}{\partial x \partial t} \right.$$
$$\left. - \overline{Q_x}(\eta, y) \frac{\partial w(\eta, y)}{\partial t} \right] \mathrm{d}y$$
$$= \frac{8\alpha^2 \sqrt{1 + \alpha}\, k_f^3}{1 - \alpha^2} |A_0|^2$$

$$= \frac{2\sqrt{1 + \alpha}(1 - \nu - \alpha)^2 k_f}{(1 - \alpha^2)^{3/2}} \left| \frac{A}{L_-(k_f)} \right|^2$$
$$= \frac{2\sqrt{1 + \alpha}(1 - \nu - \alpha)^2 k_f^3}{1 - \alpha^2} |\mathcal{A}|^2 \quad \left(k_f = \sqrt{\frac{\omega}{\alpha}} \right). \qquad (73)$$

At the same time the crack front asymptotes are defined by the asymptotes of $M_+(k)$ ($k \to \mathrm{i}\infty$) and $\psi_-(k)$ ($k \to -\mathrm{i}\infty$) [see (68) and (70)]. These asymptotes, in the same way as the stress-displacement energy couple in elasticity, define the local energy release rate (see Slepyan 2002, p. 27, Eq. 1.42)

$$G_0 = -\lim_{s \to +\infty} s^2 M_+(\mathrm{i}s)\psi_-(-\mathrm{i}s) = (\Re A)^2$$
$$= k_f^2 \sqrt{1 - \alpha^2} \left[\Re(\mathcal{A} L_-(k_f)) \right]^2. \qquad (74)$$

We now represent the complex amplitude of the feeding wave as $\mathcal{A} = |\mathcal{A}| \exp(\mathrm{i}\phi)$, where ϕ is the 'initial' phase which defines the crack tip position relative the wave. Given the critical local energy release rate, G_c, the phase is defined by

$$\Re\Phi = \frac{\sqrt{G_c}}{k_f(1 - \alpha^2)^{1/4}|\mathcal{A}|}, \quad \Phi = L_-(k_f)\mathrm{e}^{\mathrm{i}\phi}. \qquad (75)$$

This equation also defines the lower level of the wave amplitude required for the crack to grow

$$\min|\mathcal{A}| = \frac{\sqrt{G_c}}{k_f(1 - \alpha^2)^{1/4}\max\Re\Phi}. \qquad (76)$$

Note that, since α is very close to one, the local energy release is only a small part of the feeding wave energy

$$\frac{G_0}{G} = \frac{(\Re\Phi)^2}{2k_f\sqrt{1 + \alpha}(1 - \nu - \alpha)^2}$$
$$\approx \frac{(\Re\Phi)^2}{v^2\sqrt{\omega}}(1 - \alpha)^{3/2}. \qquad (77)$$

6.5 Antisymmetric mode

Now, we consider the antisymmetric problem, $w(\eta, -y) = -w(\eta, y)$. The corresponding conditions at $y = 0$ are

$$w = M_y = 0 \ (\eta > 0), \quad M_y = Q_y = 0 \ (\eta < 0). \qquad (78)$$

In the same way as for the symmetric problem, we come to the equation similar to (61) but with respect to the energy pair $Q_+(k)$, $w_-(k)$

$$Q_+(k) - L_a(k)w_-(k) = 0, \quad L_a(k) = L(k)\mu_1\mu_2, \qquad (79)$$

where $L(k)$ is defined in (62). We represent

$$L_a = L^0 l_{a+} l_{a-},$$
$$l_{a+} = l_+ \sqrt{[0 - i(k - v)][0 - i(k + v)]},$$
$$l_{a-} = l_-(0 + ik). \tag{80}$$

Using the relation of the same type as in (69) we find the local energy release rate for this hyper-singular mode

$$G_{a0} = -\lim_{s \to +\infty} s^2 Q_+(is) w_-(-is) = (\Re A)^2. \tag{81}$$

Furthermore, similar to the relation (72), we have

$$A_{a0} = \frac{A(1 - v - \alpha)}{2\alpha L_-(k_f)},$$
$$\mathcal{A} = -A_0 \frac{2\alpha}{1 - v - \alpha}$$
$$= -\frac{A}{L_-(k_f)}. \tag{82}$$

From this and (73) it follows that the energy delivered by the feeding wave per unit length of the crack path is

$$G_a = \frac{8\alpha^2 \sqrt{1 + \alpha}\, k_f^3}{1 - \alpha^2} \,|A_0|^2$$
$$= \frac{2\sqrt{1 + \alpha}\,(1 - v - \alpha)^2 k_f^3}{1 - \alpha^2} \left| \frac{A}{L_-(k_f)} \right|^2$$
$$= \frac{2\sqrt{1 + \alpha}\,(1 - v - \alpha)^2 k_f^3}{1 - \alpha^2} \,|\mathcal{A}|^2 \quad \left(k_f = \sqrt{\frac{\omega}{\alpha}}\right). \tag{83}$$

Now the energy ratio is [compare with (77)]

$$\frac{G_{a0}}{G_a} = \frac{(\Re \Phi)^2}{2k_f^3 \sqrt{1 + \alpha}\,(1 - v - \alpha)^2}(1 - \alpha^2)$$
$$\approx \frac{(\Re \Phi)^2}{\sqrt{2}\, v^2 \omega^{3/2}}(1 - \alpha) \quad (v > 0). \tag{84}$$

Thus, this continuous model as a waveguide for the edge wave satisfies the necessary conditions allowing for the crack to propagate uniformly under the localized wave. Recall, however, that contrary to the lattice, the plate dispersion relations define a unique crack speed independently of the wave amplitude, and this relations give no direct evidence concerning the existence of other ordered regimes.

7 Conclusions

In this paper, it is shown how the dynamic fracture can grow in an acoustic waveguide under a localized harmonic wave. The steady-state regime is described for a lattice and a continuous material model. We have considered mode III fracture in the square lattice as the simplest model of such a kind. A similar way of the considerations can be used for the other fracture modes based on different lattice structures.

The crack-speed oscillation regimes found in numerical simulations of the lattice received some theoretical justification. Note that the crack was assumed to grow along a strait line. This implies that in the lattice the ratio of the strength of crack-path breaking bonds to the that of the parallel-to-the-crack bonds is low enough. Otherwise, the latter bonds can break as it was shown by Marder and Gross (1995) for a uniform lattice.

In the lattice, depending on the interface contrast, both subsonic and supersonic crack speeds can exist, while the feeding (driving) wave is localized. In both problems, in the lattice problem as well as in the flexural plate one, the wave features have basic meaning, and the wave dispersion relations play the key role.

The feeding and dissipative (reflected) waves are still localized in the case of a low contrast interface as well as for the high contrast one. However, the energy radiated from the interface increases greatly as the contrast decreases.

With respect to the lattice it is of interest that the cluster-type wave representation, suggested in the present paper, yields that maximal speeds agree with the average crack speeds found in the numerical simulations. It is shown that such a representation can also provide insight for evaluation of the local crack-speeds within the cluster.

In the case of the flexural plate, where the crack can grow uniformly subject to the loading by the edge wave, the dispersion relations give the uniquely defined crack speed, which is frequency-dependent but wave-amplitude-independent.

References

Marder M, Gross S (1995) Origin of crack tip instabilities. J Mech Phys Solids 43:1–48

Mishuris GS, Movchan AB, Slepyan LI (2009) Localised knife waves in a structured interface, J Mech. Phys. Solids (to appear)

Slepyan LI (1981) Crack propagation in high frequency lattice vibrations. Sov Phys Dokl 26:900–902

Slepyan LI (2002) Models and Phenomena in Fracture Mechanics. Springer, Berlin

Slepyan L, Dempsey J, Shekhtman I (1995) Asymptotic solutions for crack closure in an elastic plate under combined extension and bending. J Mech Phys Solids 43(11):1727–1749